

THIRTEENTH EUROPEAN ROTORCRAFT FORUM

Paper No. <sup>64</sup>33

AEOELASTIC PREDICTION  
OF ROTOR LOADS IN FORWARD FLIGHT

Bernadette PELEAU and Didier PETOT  
Office National d'Etudes et de Recherches Aeronautiques  
Châtillon, FRANCE

September 8-11, 1987

Arles, FRANCE

ASSOCIATION AERONAUTIQUE ET ASTRONAUTIQUE DE FRANCE

**AEROELASTIC PREDICTION OF ROTOR LOADS IN FORWARD FLIGHT**  
Bernadette Peleau and Didier Petot  
Office National d'Etudes et de Recherches Aerospatiales  
Châtillon, France

**ABSTRACT**

A new, simple and fast calculation of the forced response of a helicopter blade in forward flight is presented with an application to the case of a flight test. The code is a step by step solution of the aeroelastic equations obtained when coupling the unsteady aerodynamics of the ONERA dynamic stall model with a modal representation of the structure. The periodic response of the blade is reached after several revolutions.

Comparisons of theoretical predictions with data from the SA 349 GV helicopter flight tests performed by Aerospatiale are shown. Influence of some of the parameters in the code is considered :

- results obtained with the unsteady aerodynamic model are compared to quasi-steady aerodynamics.
- sensitivity of the agreement between prediction and experiment is described as a function of the number of elastic blade modes.
- an improvement is attempted by adding the effect of blade vortices to the Meijer-Drees inflow model.

**1. INTRODUCTION**

Because of blade rotation and rotor translation, the equations that model the behaviour of a helicopter in forward flight have periodic coefficients. If stall is taken into account, they are also non linear. Even with 2D aerodynamics, lift and moment have to be evaluated at several blade sections, since each radius sees a different flow. Thus the use of the ONERA dynamic stall model brings a great many unknowns to the problem.

A direct method of resolution would call for the linearization of the equations about the periodic solution for the system, followed by a Floquet Analysis. This approach has been used in reference 1. Although this method gives a lot of informations about the system, it requires a good deal of computation time: proportional to  $n^3$ , where  $n$  is the number of blade sections.

There exists a simple method for solving equations, which transcends complexities: direct time integration which

requires computing time roughly proportional to  $n$ . Although we are interested in the periodic response of the rotor rather than in a transient response, this method was tried, for the following reasons:

- A high level of damping is expected, brought about by
  - the ONERA Dynamic Stall Model (including in pitch)
  - the lead-lag damper (in fact, this damper happens to be a little insufficient)
  - the flapping rate
- Unstable or poorly stable systems are mostly beyond the scope of this method.
- The ONERA stall model is quite well adapted to time step integration.
- With this method, the system remains open to many improvements (new terms in the equations, non linearities.)
- Transient responses (gusts) can easily be studied.

Thus, this method is very attractive. It has no other convergence problems than waiting for the damping out of the movements toward the periodic response. A time step integration code has been written and denoted PAP ("Pas A Pas": step by step, in French). It will be shown later that the code is not as ideal as described here: the computation time is longer than expected.

The results given by this code have been compared to in-flight measurements conducted on an Aerospatiale SA 349 Gazelle. This data (ref. 9) has been used by several authors in order to test their respective codes (ref. 2,3,4), and is thus of great interest. After obtaining the first results, it was decided to couple PAP with the non uniform inflow calculated by the METAR(AS) code. This code, recently written by Toulmay from Aerospatiale, is as yet unpublished.

## 2. DESCRIPTION OF THE PAP ANALYSIS

### Mechanics

The derivations and complete developments of the equations can be found in reference 1. Lagrange equations have been applied to the rotor with the following hypothesis (figure 1).

- The rotor does not vibrate and its rotational speed  $\Omega$  is constant.
- The blade has flap, pitch and lead-lag hinges placed in this order from the hub center outwards.
- The blade is assumed to be a flexible beam whose deflections are given as a superposition of cantilevered beam modes at  $\Omega=0$  rd/s. The classical assumption is made that the blade does not stretch through its vibratory motion.

The equations are written for one blade. Their final form is (equation 6.1 of ref.1):

$$(1) \quad M(t) \cdot \ddot{q} + B(t) \cdot \dot{q} + K(t) \cdot q = f(t) + \sum_i (C_{L_i} \cdot W_i(r_i, t) + C_{M_i} \cdot \theta_i(r_i, t))$$

where  $C_{L_i}$  and  $C_{M_i}$  are the lift and moment coefficients given by the aerodynamic model at the blade section  $i$  and  $q$  is a state vector determined by the rotor geometry:  $q = (\beta, \delta, s_1, s_2, \dots, s_m)$ , where  $\beta$  and  $\delta$  are the flap and lead-lag hinge angles, and  $s_1, s_2, \dots, s_m$  the generalized coordinates of the  $m$  elastic blade modes.

### Aerodynamics

Over the past years, a dynamic stall model has been developed at ONERA (ref.5,6,7). It uses a 2D approach in which the position of the airfoil relative to the fluid is related to the lift or moment through differential equations. The position of the airfoil is defined by the variables  $i_0$  and  $i_1$ , where  $i_0$  is the configuration where each point along the chord sees the flow with the same angle of attack, and  $i_1$  is the configuration where this angle of attack is proportional to the distance to the quarter chord, as described in figure 2.

Experience led to the adoption of the following system of differential equations as it happened to be quite successful:

$$(2) \quad \begin{aligned} \text{Lift} &= \frac{1}{2} \rho S V^2 (C_{L1} + C_{L2}) \\ \dot{C}_{L1} + \lambda \cdot C_{L1} &= \lambda \cdot C_{L1} \Big|_{i_0} + \lambda \cdot s \cdot i_1 + \sigma \cdot \dot{i}_0 + s \cdot \dot{i}_1 \\ \ddot{C}_{L2} + a \cdot \dot{C}_{L2} + r \cdot C_{L2} &= -(r \cdot \Delta C_{L1} \Big|_{i_0} + E \cdot \dot{i}_0) \end{aligned}$$

$$(3) \quad \begin{aligned} \text{Moment} &= \frac{1}{2} \rho S b V^2 (C_{M1} + C_{M2}) && (b = \frac{1}{2} \text{ chord}) \\ C_{M1} &= C_{M1} \Big|_{i_0} + s \cdot i_1 + \sigma \cdot \dot{i}_0 + s \cdot \dot{i}_1 \\ \ddot{C}_{M2} + a \cdot \dot{C}_{M2} + r \cdot C_{M2} &= -(r \cdot \Delta C_{M1} \Big|_{i_0} + E \cdot \dot{i}_0) \end{aligned}$$

$\lambda, s, \sigma, r, a, E$  are parameters deduced from wind tunnel tests. They do not have the same value for lift and moment. They depend on Mach number and on angle of attack in the stall domain.  $C_{L1}, \Delta C_{L1}, C_{M1}, \Delta C_{M1}$  are defined in figure 3. Though a stall delay can be used in this model, it has not been applied here.

### Induced velocity

An induced velocity on the whole rotor disk is necessary in order to introduce the real aerodynamic angle of attack seen by the blade sections. The Meijer-Drees formula was at first used (ref.8) but experience showed the

necessity to take into account a much finer definition of this velocity. The METAR(AS) code developed by Toulmay was then used.

For a given blade movement, this code computes the induced velocity and the lift derived from either static polars or from the ONERA model, according to the user's needs. The model assumes that the vortex sheet is swept downward at a constant speed (the mean Meijer-Drees induced velocity).

This approach is especially useful here because the aerodynamic behaviour at 97% radius must be reproduced and 2D aerodynamics alone leads to poor results.

### Method for solving the equations

The method consists in coupling the dynamic equation (1) with the aerodynamic equations (2) and (3). When applied to the blade section  $i$ , the aerodynamic equations can be written in terms of the state vector  $q$  and its first two time derivatives:

$$(4) \quad \begin{aligned} C_{L1} &= C_{L11} + C_{L21} \\ \dot{C}_{L11} + \lambda \cdot C_{L11} &= f_{11}(q, \dot{q}) + g_{11} \cdot \ddot{q} \\ \dot{C}_{L21} + a \cdot \dot{C}_{L21} + r \cdot C_{L21} &= f_{21}(q, \dot{q}) + g_{21} \cdot \ddot{q} \end{aligned}$$

$$(5) \quad \begin{aligned} C_{M1} &= C_{M11} + C_{M21} \\ C_{M11} &= f_{31}(q, \dot{q}) + g_{31} \cdot \ddot{q} \\ \dot{C}_{M21} + a \cdot \dot{C}_{M21} + r \cdot C_{M21} &= f_{41}(q, \dot{q}) + g_{41} \cdot \ddot{q} \end{aligned}$$

Substituting for  $C_{M11}$  in equation (1) gives:

$$(6) \quad (M(t) - M_e(t)) \cdot \ddot{q} + B(t) \cdot \dot{q} + K(t) \cdot q = g(t, q, \dot{q}) + \sum_i ((C_{L11} + C_{L21}) \cdot W_i(r_i, t) + C_{M21} \cdot \theta_i(r_i, t))$$

This becomes the first equation of the following system, where the other equations come directly from aerodynamics (equations (4) and (5)):

$$(7) \quad \begin{aligned} \ddot{q} &= F_1(q, \dot{q}, (C_{L11})_i, (C_{L21})_i, (C_{M21})_i) \\ \dot{C}_{L11} &= F_2(q, \dot{q}, (C_{L11})_i, (C_{L21})_i, (C_{M21})_i) \\ \dot{C}_{L21} &= F_3(q, \dot{q}, (C_{L11})_i, (C_{L21})_i, (\dot{C}_{L21})_i, (C_{M21})_i) \\ \dot{C}_{M21} &= F_4(q, \dot{q}, (C_{L11})_i, (C_{L21})_i, (C_{M21})_i, (\dot{C}_{M21})_i) \end{aligned}$$

The problem is finally written as a first order differential equation:

$$(8) \quad \dot{Y} = F(Y) \\ \text{where } Y = (q, \dot{q}, (C_{L11})_i, (C_{L21})_i, (\dot{C}_{L21})_i, (C_{M21})_i, (\dot{C}_{M21})_i)$$

This equation is solved by a classical step by step integration method such as a fourth order Runge-Kutta or a Predictor-Corrector method. The latter is used here. The calculation begins with arbitrary initial values of the vector  $Y$  (zero for each component). The aeroelastic response of the blade is obtained for each time step. The calculation goes on during several rotor revolutions until the response becomes periodic. The periodic criterion used here is that the vector  $q$  must not vary by more than 5% after one revolution. This provides an accuracy of 0.1 degrees on flap and lag, and a very good periodicity.

The PAP code can trim the rotor by using the gradient method. In the following application, the code iterates on collective and longitudinal cyclic pitch to reach prescribed rotor drag and thrust. Generally, the rotor is trimmed after one iteration.

### Coupling with METAR(AS)

The PAP code can work with either the induced velocity given by the uniform inflow model of Meijer-Drees or the prescribed wake results given by the Aerospatiale METAR(AS) code.

The coupling between PAP and METAR(AS) is made by transferring data files from one code to the other. PAP first computes the periodic response of the blade with uniform inflow and returns the movement of the blade to METAR(AS). METAR(AS) then computes the new induced velocity which is brought back to PAP. It has been checked that the periodic response thus obtained needs no further iteration.

### Computing time

The computing time is proportional to:

- the azimuthal step size: the largest step to be used depends mainly on the higher frequency of the system. With a blade mode at  $6\Omega$ , a step of 1.5 degrees had to be used.
- the number of blade sections: 7 appears to be sufficient.
- the number of revolutions needed to obtain periodicity: the number of revolutions is determined only by the rotor and by the flight condition. It is reduced when the lightly damped lag modes can be avoided. Between 5 (rigid blade) and 60 (soft blade and high speed) revolutions were necessary.

Computing time is of the order of magnitude of 1 second for 1 rotor revolution on a Cray XMP for a full

flexible blade and unsteady aerodynamics. 1 minute is generally sufficient to obtain the periodic solution. The use of METAR(AS) adds 20 seconds to this time. The search for a trimmed solution multiplies the time by 4.

### 3. COMPARISONS WITH THE SA 349 GV FLIGHT TEST DATA

Flight tests were carried out by Aerospatiale in 1984 on the SA 349 GV Gazelle helicopter. The fully articulated hub was fitted with a non linear lag damper. The 10.5 m diameter rotor had 3 twisted rectangular blades having OA209 profiles. Structural and aerodynamic loads were measured in flight (reference 9). As the PAP code does not calculate structural loads, only the pressure measurements are of interest here. They were made at the 75%, 88% and 97% radial stations, with a set of 20 chordwise pressure transducers at each station (upper and lower surface). The obtained lift coefficients are in fact the normal force coefficients,  $C_N$ . However  $C_N$  and  $C_L$  are rather similar in this flight test.

The pressure transducer distribution was not fine enough to provide accurate  $C_N$  data, and the flapping angle had not been correctly measured. Thus in this paper, correlations can be made only with lift coefficients.

A Gaussian distribution with 7 blade sections provides results at the 77.7%, 90.3%, and 98.1% radial stations, not too far from the experimental sections at 75%, 88%, and 97% radius. No tip corrections are made in the computation. The non-linear lag damper is modeled through its mean damping and stiffness.

#### Overall results

Results and comparisons with experimental data are relative to the flight conditions presented in table 1. Rotor thrust and drag were not measured in flight. The accuracy of the measured pitch angle is questionable. Thus to calculate trim, the rotor thrust and drag, the shaft angle and the lateral cyclic pitch issued from an Aerospatiale whole aircraft analysis were used (table 2). For turning flight, the experimental data and an estimation of the rotor thrust and drag had to be used as nothing else was available.

Comparisons between measured and calculated collective and cyclic pitch and power are shown in figure 4. Collective and cyclic pitch angles from PAP are within one degree of experiment at low speeds and this difference increases to 3 degrees at higher speed. Trimmed calculations allow PAP to match the measured power.

## Blade flexibility

Several calculations with different modal representations were made. In order to make the comparison easier, the trim of the most complete calculation (7 elastic modes) gave the pitch controls for the other calculations. Figure 6 shows the periodic  $C_L$ , the flap and lag angles,  $\beta$  and  $\delta$ , and the twist at the blade tip.

- 7 mode analysis: Fig. 5 shows the first 7 cantilever blade modes measured at rest. There are 4 modes in flapping, 2 in lead-lag and 1 in torsion. On the rotor, the hinge angles  $\beta$  and  $\delta$ , add to these 7 degrees of freedom.
- 5 mode analysis: the last 2 modes are deleted and the results are unchanged.
- 3 mode analysis: only the first of flap, lead-lag and torsion modes are kept. The only significant change appears on the twist (0.5 degrees), but the mean and peak-to-peak values are unchanged. The difference might be due to the neglected torsional component of mode 4.
- single mode analysis: only torsion remains. The  $C_L$  is little affected by the limitation to one elastic mode. However a single torsional mode is not sufficient to predict adequately the flap angle and the twist.
- rigid blade analysis: all the results show that torsion is absolutely necessary. The effect of the torsional mode on the flap angle is to alter its free sinusoidal behaviour. Torsion acts as an additional pre-twist on the blade which the pilot has to account for by increasing the pitch. The effect on the results obtained with prescribed controls is a large increase in rotor thrust (33%), power (28%) and thus in blade lag.

## Dynamic stall effect

The PAP code uses the dynamic stall model developed at ONERA (ref.5,6,7) as 2D aerodynamics. Quasi-steady aerodynamics cannot be used in the present approach because there would be no damping of the torsional oscillations. The first equation in  $C_M$  :

$$(9) \quad C_{M1} = C_{M1} \Big|_{h=0} + s \cdot i_1 + \sigma \cdot \dot{i}_0 + \xi \cdot \dot{i}_1$$

of the ONERA model contains the experimental aerodynamic damping that PAP needs. The "pseudo quasi steady" calculation carried out with PAP (e.g. figure 7) denotes the



use of steady lift, and steady moment corrected by the linear aerodynamic damping of the model.

The 107, 200, and 290 km/h flight speed results show no influence of dynamic stall, due to the fact that stall domain was too limited. In order to study dynamic stall, a turning flight case was considered at a load factor of 2 and at 260 km/h. It was treated by PAP as a forward flight case with a load factor of 2 and with the measured control positions prescribed as no Aerospatale trimmed solution was available. Results are shown on figure 7.

The use of the dynamic stall makes a difference but the lift curves cannot be said to be improved. This case was studied simply to see the influence of dynamic stall, which is very low in normal flight conditions. This comparison with experimental data cannot be used to validate the dynamic stall model because:

- flight conditions are not well enough defined (descending rate / turning flight / no reliable trimmed model could be used)
- the oscillations present during the experiment had amplitudes similar to the pseudo quasi steady / unsteady differences and they can probably not be accounted for by the model. These oscillations might be due to a high torsional response. This would not be surprising since torsion is very sensitive to aerodynamic conditions. Figure 7b shows that the stall model has a large effect on the twist of the blade (amplitude and phase).

### Wake effect

METAR(AS) allows PAP to take non linear inflow into account. Figure 8 shows how this induced velocity distribution is very different from the Meijer-Drees inflow. A large vortex influence which produces the highest peak on the  $C_L$  curve (figure 9a) can be seen between azimuth 150° at 65% radius and azimuth 270° at the blade tip.

Predictions of lift coefficients from PAP with the Meijer-Drees and the METAR(AS) induced velocities (figure 9) show 3 types of improvement brought by METAR(AS):

- The peaks on experimental  $C_L$  curves due to the wake at 107 km/h and 200 km/h are predicted at the right azimuths.
- With Meijer-Drees inflow and no tip correction, the  $C_L$  at 97% radius on the retreating side is always overestimated. With METAR(AS), it is reduced to the experimental level. Thus the METAR(AS) induced velocity acts correctly as a tip correction.
- At 200 and 290 km/h, the lift prediction on the advancing side is much closer to the experimental data, especially at 88% and 97% radius.

Despite these far reaching improvements, the prediction at 75% radius is rather disappointing for 200 and 290 km/h. METAR(AS) has not been able to reproduce the large increase in lift on the retreating blade which the CAMRAD code (ref.2) attributes to a wake effect.

#### 4. CONCLUSION

The application of PAP to the SA 349 GV flight test has led to the following conclusions:

- The calculated lift coefficient curves generally predict the measured data. It seems that the mechanical and 2D aerodynamic components of PAP work correctly.
- The use of METAR(AS) brings large improvements at low speeds and is particularly successful at very low speeds. However at high speeds, the increase of  $C_L$  on the retreating blade is not correctly predicted.
- The torsional degree of freedom must be introduced. Otherwise, on this type of rotor with a  $4\Omega$  torsional frequency, rigid blade analyses have to be trimmed.
- For a rotor performance analysis, a small number of elastic blade modes are sufficient. In fact, only the first torsional mode is necessary in the present case.
- In order to predict the blade trajectory, more elastic blade modes are needed (5 in the present case).
- Even at 290 km/h, dynamic stall has no noticeable effect. It is only required in extreme flight conditions (very high speeds or high load factors). The flight condition studied here (260 km/h, turning flight) is not accurate enough to lead to clear conclusions.
- The computing time has been a little disappointing but it remains at a reasonable level so that the PAP code can be used freely for all sorts of application.
- More comprehensive measurements during recent Aero-spatiale flight tests will provide the data necessary for a more detailed validation of the PAP code.

The PAP code makes direct use of the qualities of the ONERA dynamic stall model (high speed applications) and takes advantage of its differential equation formulation. This study has shown the versatility of the code by the ease with which 2 different aerodynamic models (dynamic stall and quasi steady models) and 2 induced velocity formulations

(Meijer-Drees and METAR(AS)) are used indifferently. This code does not purport to give as accurate results as the 3D rotor codes (for example ref.10). But it is a useful tool in many cases: parametric studies, development tests and quick analyses for the industry. PAP's changeability leaves it open to many improvements.

## REFERENCES

1. C.T. Tran, D. Petot, and D. Falchero, Aeroelasticity of Helicopter Rotors in Forward Flight, La Recherche Aero-spatiale, 1982-4.
2. G. Yamauchi, R. Heffernan, and M. Gaubert, Correlation of SA 349/2 Helicopter Flight Test Data with a Comprehensive Rotorcraft Model, NASA TM 88351, Feb. 1984.
3. M. Gaubert, and G. Yamauchi, Prediction of SA 349/2 GV Blade Loads in High Speed Flight using Several Rotor Analyses, American Helicopter Society 42th Annual National Forum, Saint-Louis, Missouri, May 1987.
4. R.Heffernan, Effect of Helicopter Blade Dynamics on Blade Aerodynamic and Structural Loads, AIAA Paper No. 87-0919-CP, AIAA Dynamics Specialists Conference, Monterey, California, April 1987.
5. R.Dat, C.T. Tran, and D. Petot, Semi-Empirical Model for the Dynamic Stall of a Helicopter Blade, ONERA TP 1979-149.
6. C.T. Tran, and D. Petot, Semi-Empirical Model for the Dynamic Stall of Airfoil in view of the Application to the Calculation of Responses of a Helicopter Blade in Forward Flight, Vertica, 1981, Vol 5.
7. D.Petot, Progress in the Semi-Empirical Prediction of the Aerodynamic Forces due to Large Amplitude Oscillation of an Airfoil in Attached or Separated Flow, 9th European Rotorcraft Forum, Stresa, Italy, Sept. 1983.
8. J.M. Drees, A Theory of Airflow through Rotors and its Application to some Helicopter Problems, Journal of the Helicopter Association of Great Britain, July-Sept 1949.
9. R. Heffernan, and M. Gaubert, Structural and Aerodynamic Loads and Performance Measurements of an SA 349/2 Helicopter with an Advanced Geometry Rotor, NASA TM 88370, Nov. 1986.
10. R. Dat, and C.T. Tran, The Use of Advanced Aerodynamic Models in the Aeroelastic Computations of Helicopter Rotors, 12th European Rotorcraft Forum, Garmisch-Partenkirchen, West Germany, Sept. 1986.

speed, km/h	107	200	290	262
altitude, ft	1000	1000	1000	1000
load factor	1	1	1	2
advance ratio	0.14	0.26	0.38	0.34
thrust coefficient/solidity	0.065	0.065	0.064	0.128
weight, kg	1985	1979	1967	1951

Table 1 : Selected Flight Conditions.

speed, km/h	107	200	290
load factor	1	1	1
rotor shaft angle: $\alpha_s$ , deg	5.67	9.18	12.92
lateral cyclic pitch: $\theta_c$ , deg	0.78	1.03	1.60
rotor drag: $F_x$ , N	456	1686	3989
rotor thrust: $F_z$ , N	19244	19296	20392

Table 2 : Trimmed Inputs (from Aerospatiale code)

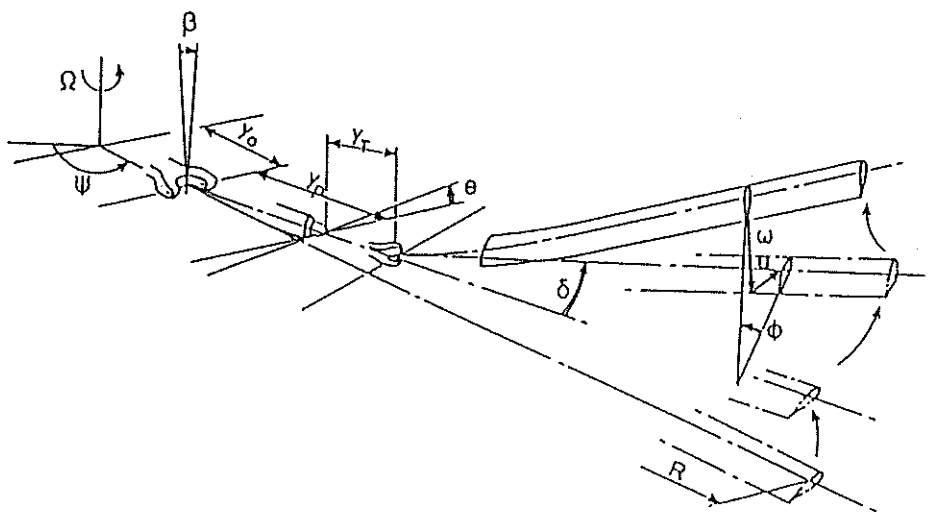


Fig :1 - Rotor Kinematics :  $\Psi, \beta, \theta, \delta, \omega, \phi$

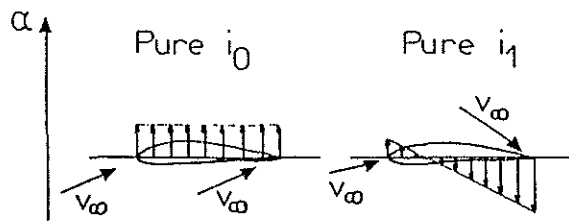


Fig:2\_ Definition of  $i_0$  and  $i_1$

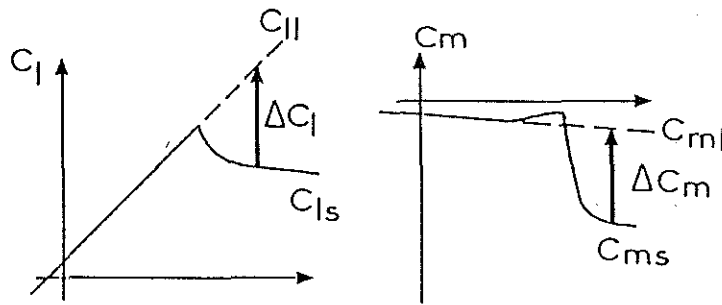


Fig:3\_ Definition of  $C_{l1}$ ,  $\Delta C_l$ ,  $C_{m1}$ ,  $\Delta C_m$  used in the dynamic stall model

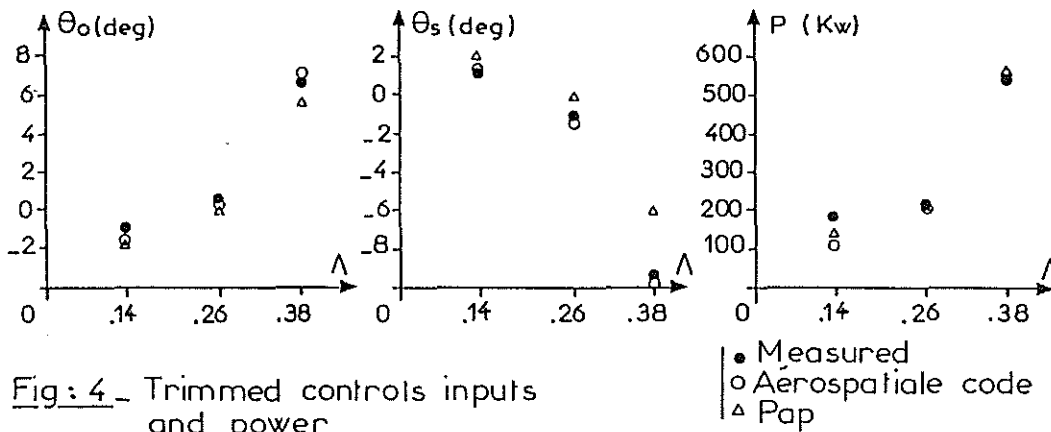


Fig:4\_ Trimmed controls inputs and power

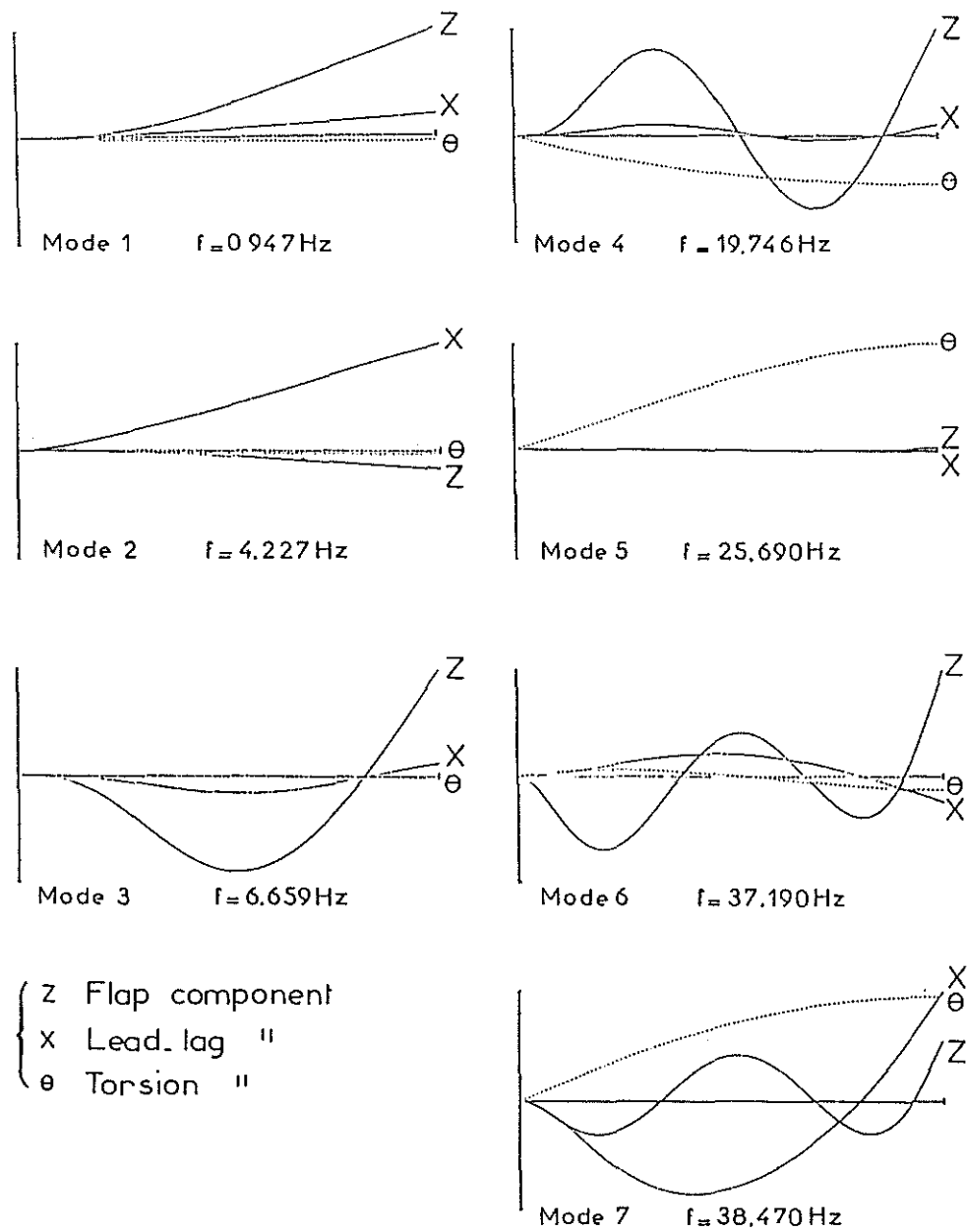


Fig:5 - Frequencies and mode shapes of a 349 GV blade at rest measured by ONERA

SPEED = 290. KM/H  
 ALTITUDE = 1000. FT  
 LOAD F. = 1.00

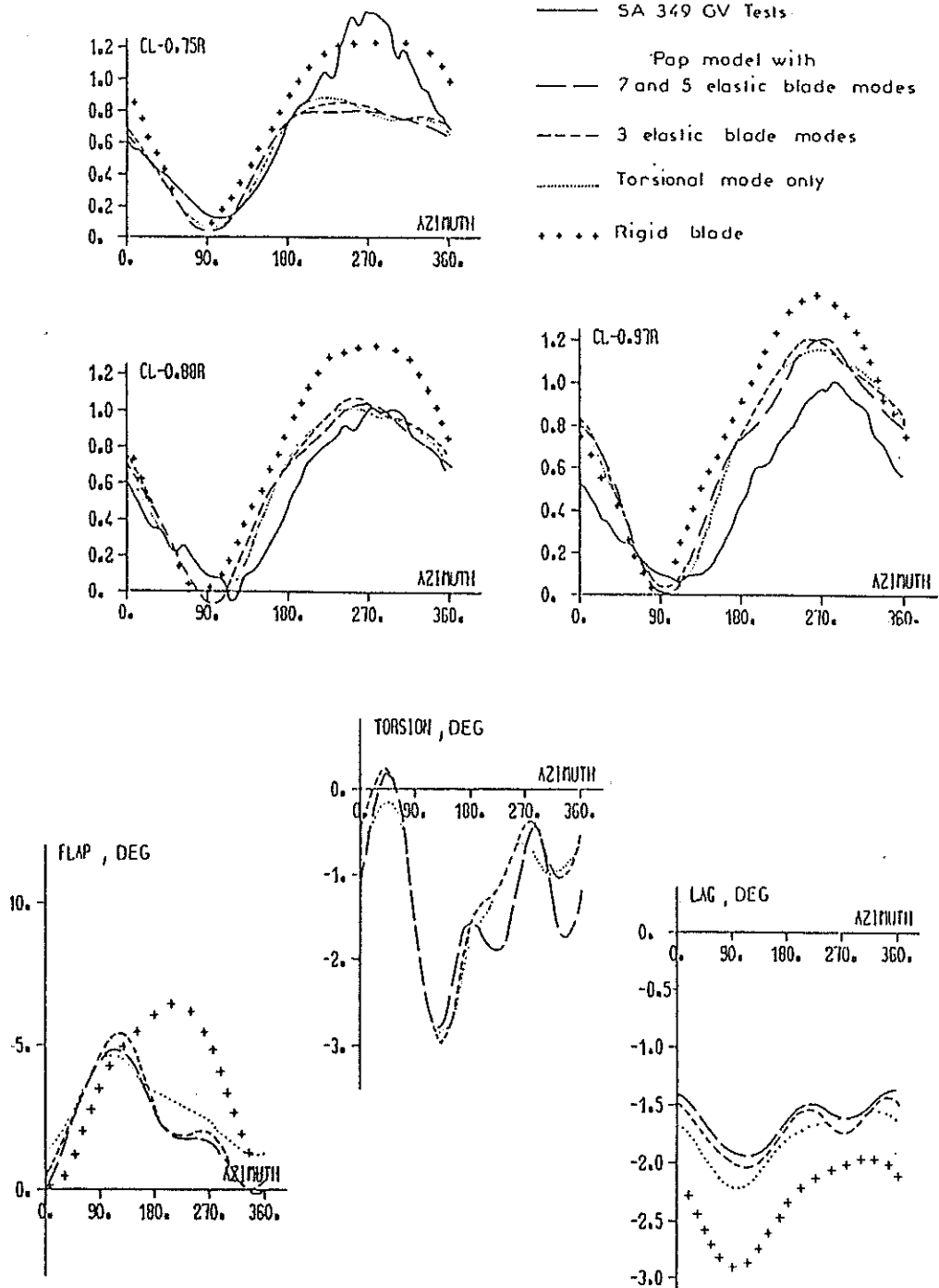


Fig:6 - Effect of blade flexibility

SPEED = 262. KN/H  
 ALTITUDE = 1000. FT  
 LOAD F<sub>z</sub> = 2.00

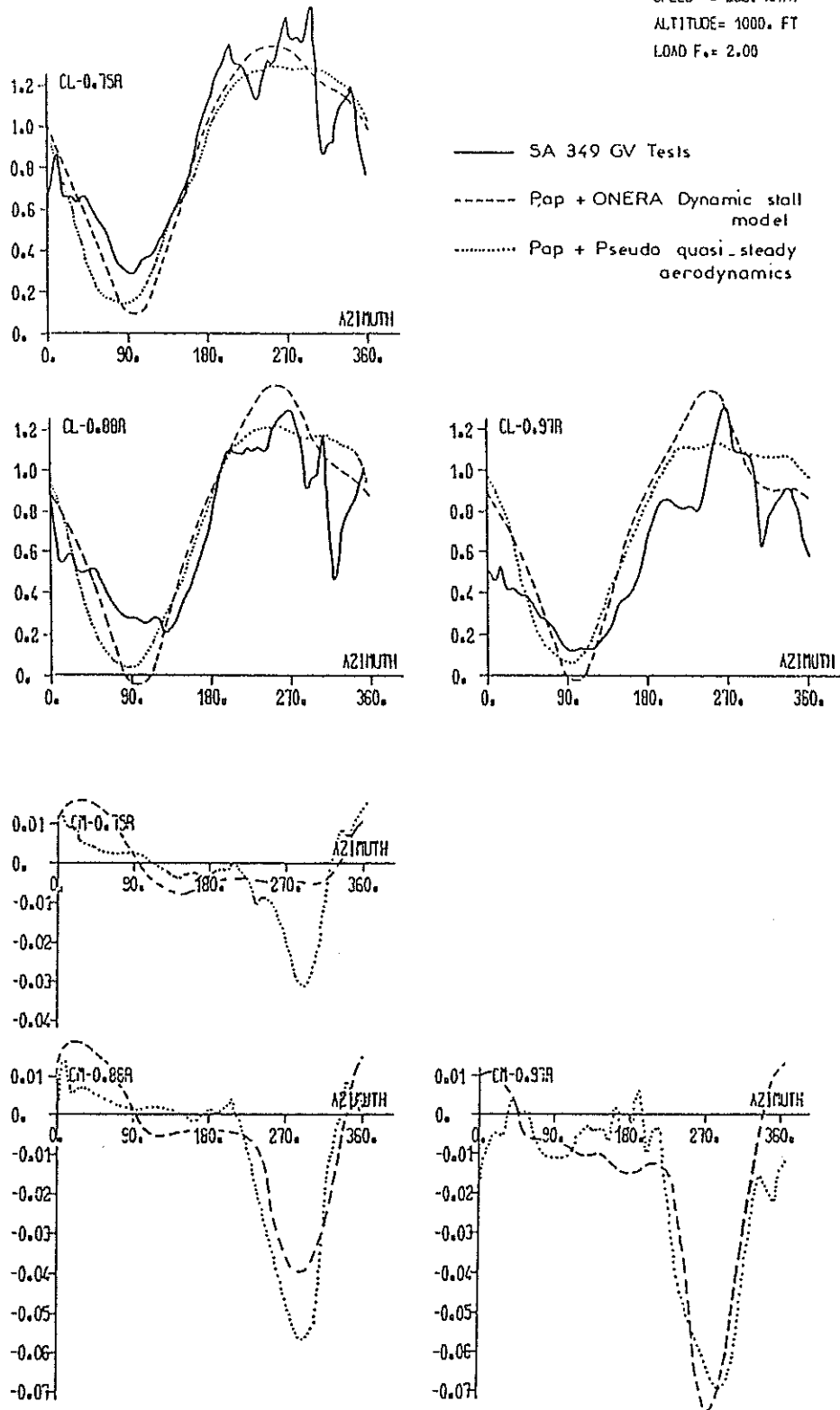


Fig.7a - Dynamic stall effect



- - - - Pap + ONERA Dynamic stall model  
 - · - · - Pap + Pseudo quasi-steady aerodynamics

SPEED = 282. KM/H  
 ALTITUDE = 1000. FT  
 LOAD F. = 2.00

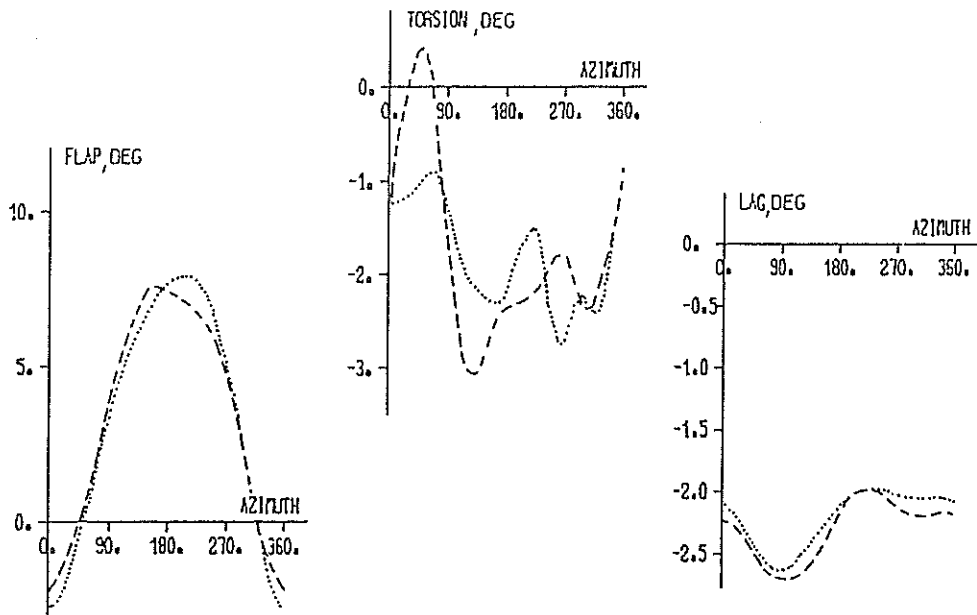


Fig:7b - Dynamic stall effect

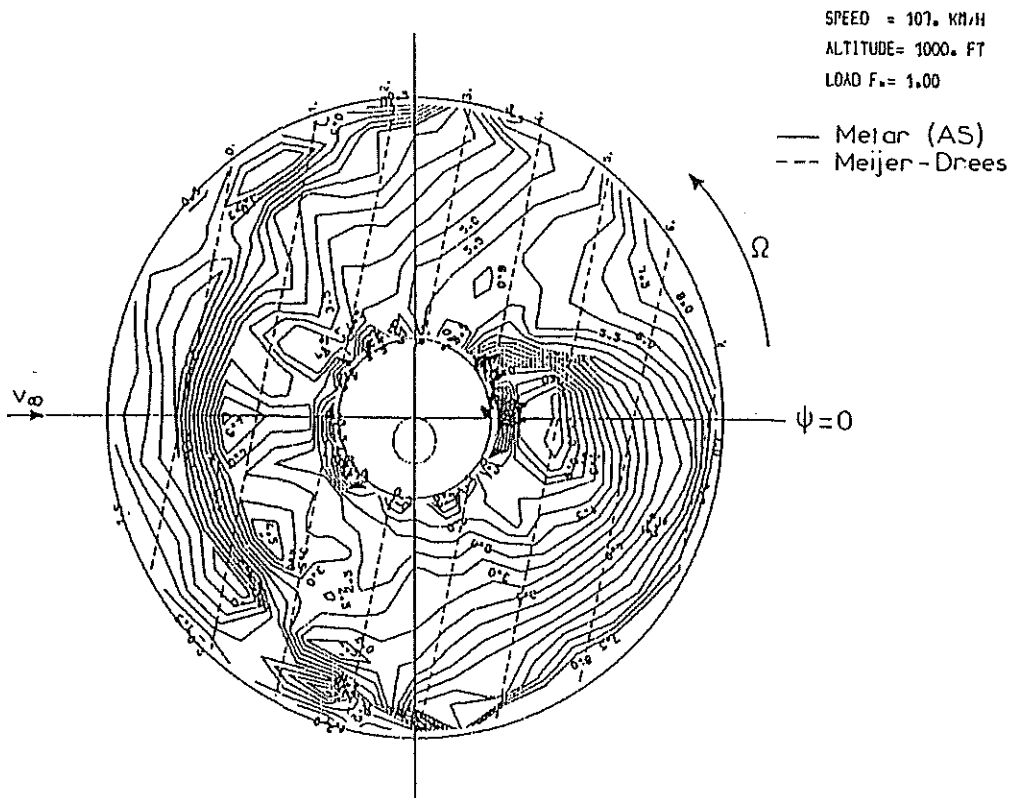
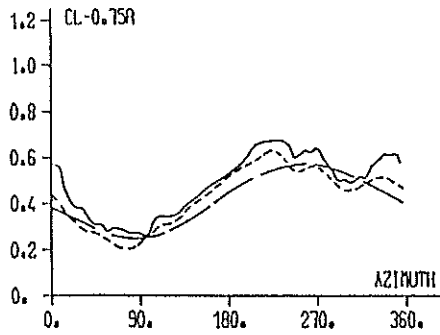
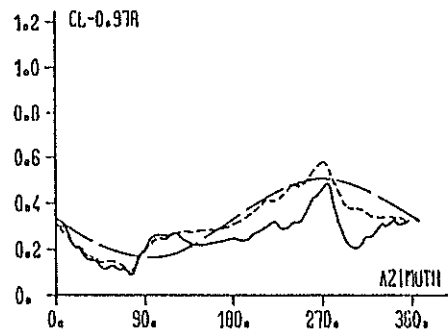
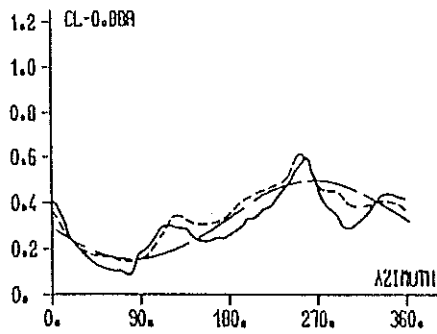


Fig:8 - Meijer.Drees and Mejar(AS) induced velocities (m/s)

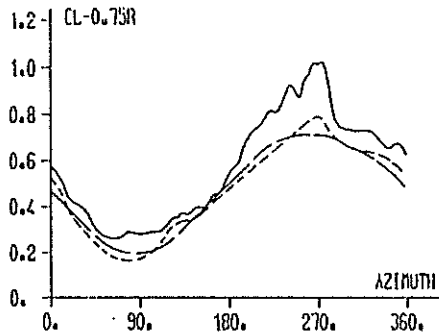
SPEED = 107. KM/H  
 ALTITUDE = 1000. FT  
 LOAD F<sub>w</sub> = 1.00



— SA 349 GV Tests  
 - - - Pap + Metar (AS)  
 - · - Pap + Meijer-Drees  
 [Trimmed Models]



SPEED = 200. KM/H  
 ALTITUDE = 1000. FT  
 LOAD F<sub>w</sub> = 1.00



— SA 349 GV Test  
 - - - Pap + Metar (AS)  
 - · - Pap + Meijer-Drees  
 [Trimmed Models]

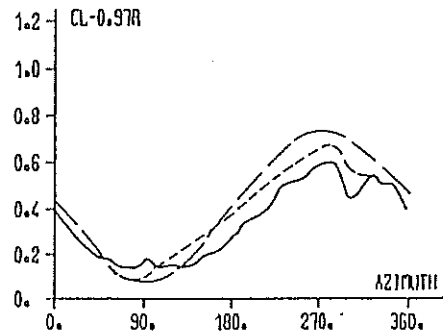
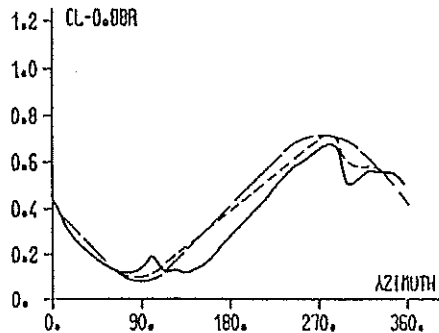
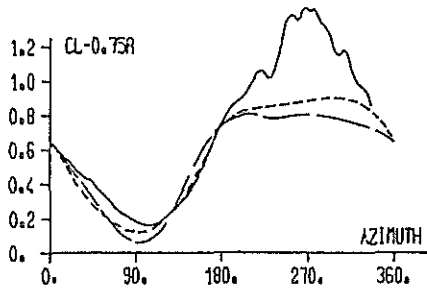


Fig 9a - Wake effect

SPEED = 290. KM/H  
ALTITUDE = 1000. FT  
LOAD F. = 1.00



— SA 349 GV Tests  
- - - Pap + Melar (A5)  
- · - Pap + Meijer Drees  
[Trimmed Models]

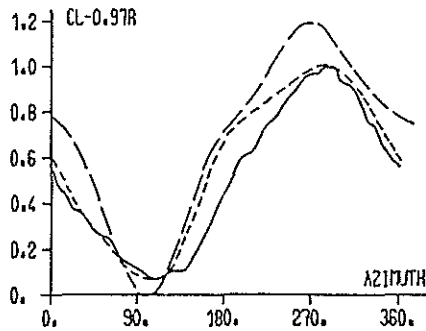
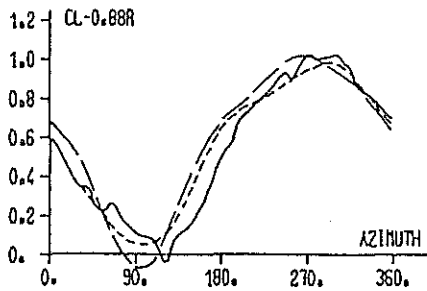


Fig:9b - Wake effect